DOI: 10.13009/EUCASS2017-38

Experimental characterization of the acoustics of the future Ariane 6 launch pad

P. Malbéqui, R. Davy, C. Bresson
DAAA, Aerodynamics, Aeroelasticity, Acoustics Department
Onera, 29 avenue de la Division Leclerc, 92322 Châtillon Cedex, France

Abstract

This paper describes the characterisation of the jet noise on the preliminary design of the launch pad dedicated to the future launcher Ariane 6. The assessment is conducted through a tests campaign carried out at the Martel facility, with a mockup of the launch pad at 1/40-scale. In addition to the acoustical measurements around the fairing, a 115-microphone phase array provides the localization of the noise sources on the launch pad. The semi-empirical code Minotaure finds the efficiency of the trenches covering at the reduced scale and provides the jet noise environment on the Ariane 6 launcher at full scale.

1. Introduction

At lift-off, the jet noise generated by the motors of heavy launch vehicles produces a severe environment where the loads induced may damage the payload and equipments. Powerful launch vehicles involve an increase of the external sound pressure level, where the specifications of the satellites covered by the fairing have to be accurately fulfilled. As a result, the environment of the launcher, mainly related to the jet noise and the blast wave generated at the ignition of the solid rocket motor, has to be accurately controlled and the acoustic level lowered, when necessary. This paper concerns the characterisation of the jet noise on the preliminary design of the launch pad dedicated to the future launcher Ariane 6. This activity is carried out under a programme of, and funded by, the European Space Agency. In practice, according to the expected acoustical power radiated by the jets of Ariane 6, which can be straightforwardly estimated from the kinematic energy delivered by the engines, a well-designed launch pad is required to prevent high level on the fairing during the lift-off phase.

A significant savoir faire on the characterization of the environment of the launchers at lift-off has gained from the launchers development during the last decades. In particular, in the framework of the Ariane programme, complementary technologies have been implemented for studying the jet noise and the blast wave. The available tools include both theoretical and experimental facilities. Tests, using a solid rocket motor generating a hot and supersonic jet as well as the blast wave at the very first time of the ignition, can be performed in Centre Fauga Mauzac of Onera [1]. The measurements with a propellant engine provide realistic conditions to simulate representative jet noise and blast wave. However, these tests campaign remain expensive, reducing the number of runs, and are preferably used to reinforce the design of the launch pad, when necessary. As an alternative, the Martel facility, funded by CNES and operating since 1996, dedicated to research activities on hot supersonic jets and blast wave can be used. A large amount of test campaigns have been carried out on noise radiated by free jet, impinging supersonic jet and water injection in presence of a trench. The development of the blast wave generator working at cold gas and hot gas based on methane-air combustion constitutes a powerful system generator in this facility [2]. The blast wave is produced by the deflagration of methane-air mixture ignited inside a spherical volume, under pressure up to 100 bars at a temperature of about 2500 K. Concerning the modelization, while the existing theory on the supersonic jet noise in free field is well documented by Tam [3], the semi-empirical approach derived from the standard Eldred's formulation allows to handle the complex geometry of the launch pad [5]. Increasing progress are to be underlined in Computational Fluid Dynamics on the computations of supersonic hot jet, where the Large Eddy Simulation generates the noise sources in the jet and the coupling with Computational Aero-Acoustics provides the noise radiated in the far field [6], [7]. Nevertheless, CFD requires further studies to accurately handle the complex geometry of a complete launch pad.

This study focuses on the assessment of the jet noise while the expected impact of the blast wave should be reduced. Due to the symmetry of the launch pad, the arrival time of the two blast waves on the fairing, propagating from the two ducts (Duct Over Pressure), should be about the same and this situation minimizes the sharping efforts on the fairing. In practice for the present study, the jet noise assessment is conducted through a tests campaign carried out at the Martel facility, which is an experimental bench operated by Pprime Institute. In addition to the analysis of the

DOI: 10.13009/EUCASS2017-38

acoustical measurements upstream the jet, ONERA has implemented acoustical sources localization on the launch pad and conducted semi-empirical predictions using the code Minotaure. The present study aims at evaluating the efficiency of trench covering and the influence of the water injection on the noise reduction, as function of the altitude of the launcher and to point out the acoustical sources responsible of the radiated field pressure on the fairing.
Section 2 shows the mockup geometry of the launch pad, describes the tests in the Martel facility and illustrates results on the jet noise radiated around the fairing. Section 3 concerns the identification of the noise sources using a microphone phase array, including the interest of the DAMAS technique and the geometry of the antenna set up in the Martel facility. Section 4 shows the semi-empirical Minotaure predictions on the Martel configuration and on the Ariane 6 at scale 1.

2. Tests in the Martel facility

2.1 Mockup and instrumentation set up at Martel faciliy

The Martel facility has been developed in 1996 as part of the Research and Technology CNES program. The research group AEID (Acoustique et Environnement Induits au Décollage) was created in 1990 to understand the noise radiation mechanisms associated with hot supersonic jets and to design noise reduction systems. It was composed by ASTRIUM, CEAT/MARTEL from University of Poitiers, CNES, ECL, ONERA and Pprime. In this frame, number of experiments carried out in MARTEL facility allowed us to develop semi-empirical methods and to validate numerical simulations. The MARTEL facility produces subsonic or supersonic jets, cold or hot, and is used to carry out both fundamental and applied research studies. Efficient systems to reduce the jet noise have been designed and assessed, including the water injection in the launch pad together with the trench extension [8]. The facility is characterized by a testing hall surrounded by a huge anti-noise embankment, with an efficient acoustic treatment to ensure a semi-anechoic ambience (Figure 1). The supersonic hot jet is generated by the combustion of an air-hydrogen mixture, reaching a 1600 m/s velocity and a 1700 K temperature. The nozzle used for the tests campaign is a cone-shaped convergent-divergent with an exit diameter D of 60 mm. The 1/40 scale corresponds to the ratio of D and the nozzle exit diameter of the solid rocket booster at full scale. The combustion engine and nozzle set is covered by a 2 meters high and 0.25 m diameter cylindrical fairing. The ensemble hanged at the center of a frame can vertically moves, allowing the distance between the nozzle exit to the table of the launch pad, *i.e.*, the altitude of the launcher, to vary from 0 to 40D.

Figure 1: Martel facility in Pprime

Recently, in order to pre-design the launch pad of the future Ariane 6, dedicated test campaigns have been performed at Martel, in the framework of the ADEL Research group [9]. Tests have been carried out on a modular duct, varying its section, length, depth and coverage. It was found that the more efficient covered duct (respectively open duct), to attenuate the radiated field is the deepest one (respectively longest one).
Figure 2 displays the launch pad of Ariane 6, at 1/40 scale, set up in the Martel facility. Its geometry is based on the outputs of the ADEL research. The launch pad of Ariane 6 consists of two covered, long and deep trenches. The trenches are located in opposite directions and they guide both the jets generated by the solid rocket boosters and the main cryogenic engine. At the bottom of the trenches junction, a deflector splits the jet from the cryogenic engine into the two trenches. The mockup simulates most of the Ariane 6 pad geometry, including the launch pad elements, a large plane plate representing the ground and the water injection devices located inside the flue and on the launch

DOI: 10.13009/EUCASS2017-38

table. One single jet is available in Martel facility. Then, for most of the runs, a plate of separation is located inside the launch pad, so that the jet only penetrates into one trench, while the reflections of the sound waves may come from the whole geometry of the launch pad, including the two trenches.

Figure 2: Reference mockup, set up in the Martel facility

The acoustic measurement instrumentation includes a cylindrical array composed of 6 rings, G1 to G6, of 4 microphones surrounding the combustor fairing, which simulates the launcher, as displayed in Figure 3. As detailed in Section 3, a 115-microphone phase array is also located on the ceiling of the Martel facility for the identificaction of the sound sources.

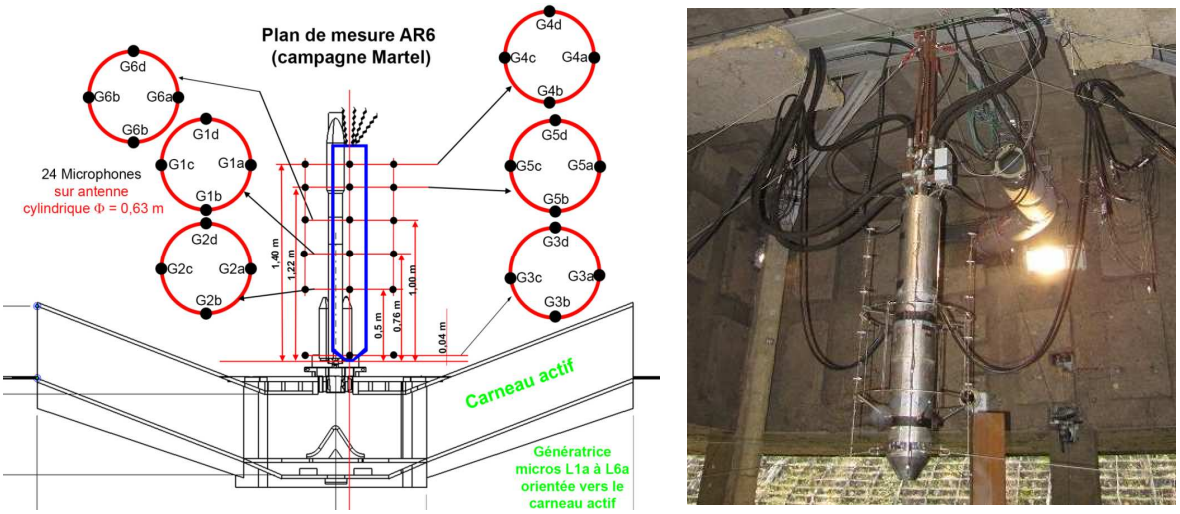

Figure 3: Microphones surrounding the combustor fairing

2.2 Sound pressure function of the launcher altitude

During the tests campaign, a large set of parameters have been assessed. They mainly concern the length and shape of the trenches and the water injection parameters. Figure 4 shows two geometries of the trench studied in addition to the reference geometry: a configuration with a shorter length compared to the reference and another one corresponding to the reference geometry with a flue extension. Figure 5 shows the overall sound pressure level averaged on the upper rings G5 and G4, as function of the altitude of the launcher for the three configurations of the trench. The general shape of the curves are characterized by: i) a significant reduction of the noise level at low altitude due to the attenuation by the covered trench, ii) a maximum of the noise level at about 20*D*, iii) an asymptotic level at 35D where the free field jet noise radiation is reached (*i.e.*, no more penetration of the jet in the

DOI: 10.13009/EUCASS2017-38

trench and weak acoustical reflections on the launch table). It is observed that, the shorter trench provides less attenuation at low level while the higher altitude finds stronger levels, the slope of the trench being more pronounced and, as a result, the acoustical reflections towards the fairings more intense. The configuration with the trench extension finds a similar behavior to the reference one, with few additional attenuation at low altitudes from 0 to 5*D*. Finally, according to these results the geometry considered is the reference one in Figure 2.

Short trench Reference trench with an extension

Figure 4: Geometries of the trenches

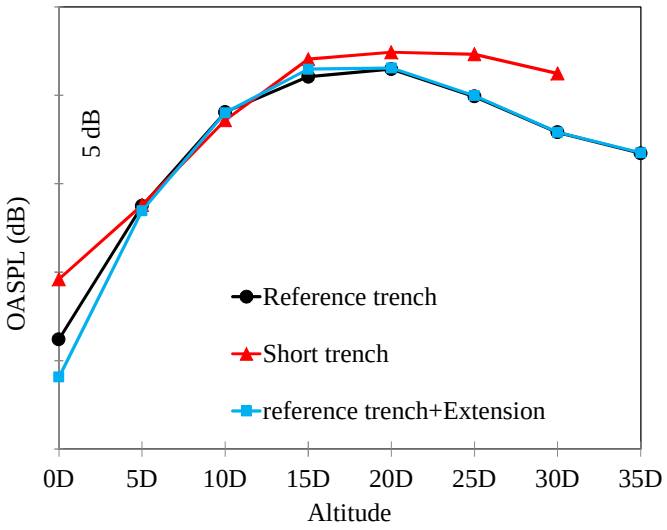

Figure 5: Sound pressure level on the fairing

In order to reduce the radiated field, three kinds of device of water injections have been implemented on the launch pad, as shown in Figure 6. The first water injection device in Figure 6a is composed by 4 nozzles located at the entrance of the trench and inside it. The second one in Figure 6b is composed by a ramp of nozzles so that the water deluge is injected above the launch table. The third one in Figure 6c is made of 4 ramps of nozzles surrounding the launch table and debiting outwards. The two first devices aim at reducing v, the velocity of the supersonic jet, to reduce the sound pressure level related to v^3. The third device aims at creating a water curtain between the acoustics waves reflecting on the launch pad and the radiated field on the fairing. The angle of the nozzles, the shape of the nozzles cylindrical or plan are the main parameters for this study of the water injection devices. Typically the mass flow of each water injection device can goes from 1 to 4 kg/s while the mass flow of the supersonic jet equals to 1.2 kg/s. During a run, while the supersonic jet is debiting, the following sequence for the water injection is achieved: dry configuration, water injection alone at the entrance of the trench, deluge above the table and deluge outwards the table. Figure 7 illustrates the influence of the water injection on the radiated sound pressure for the reference trench configuration. It is found that a significant level attenuation of about 6 decibels is obtained at low altitudes by the water injection at the entrance of the trench (red curve) and that a reduction level from 1 to 3 decibels can be reached, in the altitudes range 5*D* to 25*D* using the deluge above the launch table (blue curve). As plotted on the

DOI: 10.13009/EUCASS2017-38

green curve, for altitudes 5*D* to 15*D*, considering together the water injection at the entrance and the deluge above the table gives a similar effect to the deluge alone, suggesting that the water injection at the entrance is no more efficient up to 5*D*. Finally, it was found that the deluge of water curtain outwards the launch table does not provide significant additional attenuation.

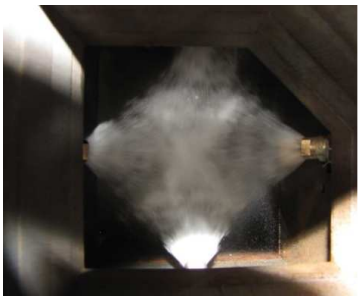

a) Water injection at the trench entrance

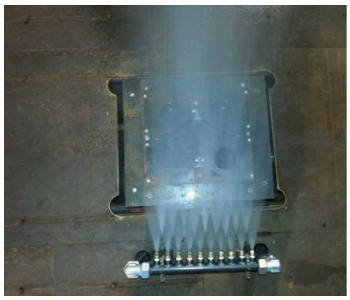

b) Water deluge above the launch table

c) Water deluge outwards the launch table

Figure 6: Water injection devices implemented on the mockup of the launch pad

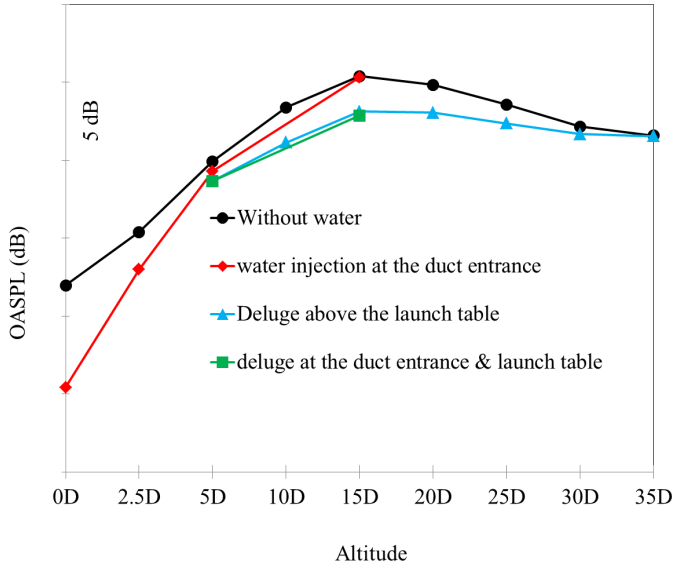

Figure 7: Influence of the water injection

3. Identification of the noise sources on the launch pad

In free field, the upstream radiation of the supersonic jet is described by three components: the turbulent mixing noise, the broadband shock noise and the screech tone, see Figure 8a. The turbulent mixing component mainly radiates downstream the jet (Figure 8b). The physical mechanism of these components is well established and documented by Tam [3]. In the presence of the launch pad, the configuration is much more complex. Figure 8c displayed a schematic diagram of the intending acoustical waves radiating upstream, in the fairing direction. At low altitudes of the launcher during the lift-off phase, typically 0 to 30*D*, the screech and tone noise still radiates upstream, while the three following sources can also contribute: i) the turbulent mixing noise emitted downstream the jet and reflecting on the launch table, ii) the acoustical waves radiated at the exit of the trench and iii) the additional sources generated by the impacts of the jet on the launch table. The radiation efficiency of these sources strongly depends upon the altitude of the launcher. This section proposed to study the performance of the phase array techniques to localize the sound sources in such a complex situation of the supersonic jet impacting the launch pad.

DOI: 10.13009/EUCASS2017-38

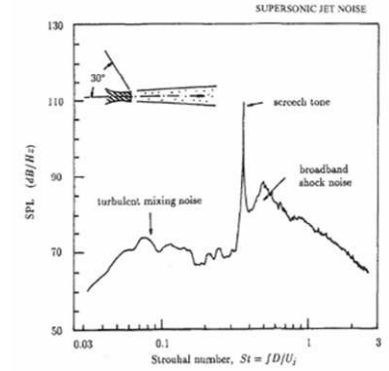

a) Upstream radiation in free field [3]

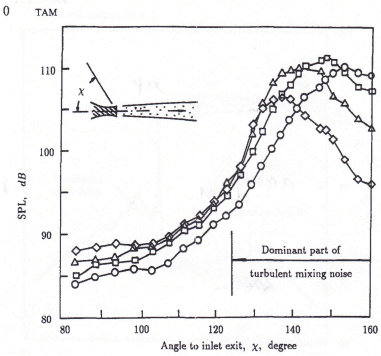

b) Noise directivities at seleceted Strouhal number [4] (○) St = 0,067; (□) St= 0.12; (Δ) St= 0;20; (◊) St = 0,40.

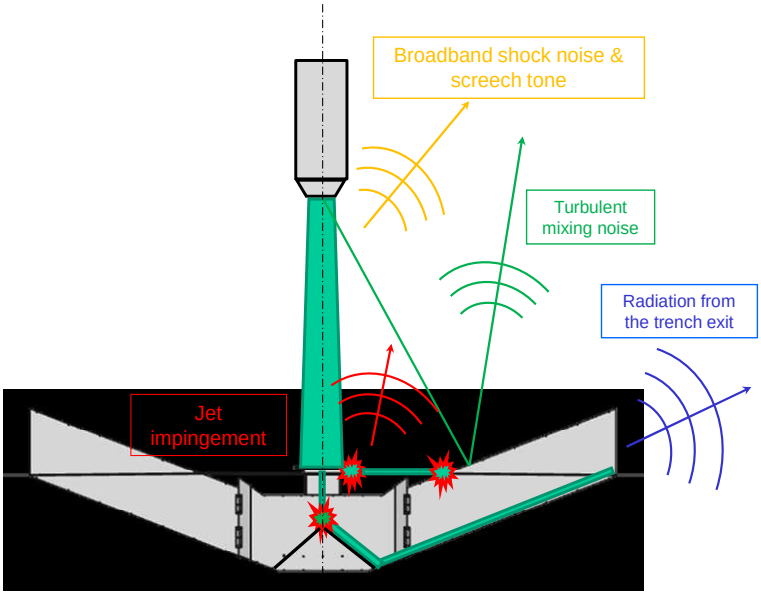

c) Intending acoustical sources on a the launch pad

Figure 8: Noise radiation of a supersonic hot jet

3.1 Identification of noise sources with a microphone phase array

First attempts of noise sources localization in the aerospace industry rely on the Conventional Beam Forming (CBF). In the principle of the CBF, the microphone signals are delayed in time, weighted by and amplitude factor and then added together over the N_M microphones of the array. Schematically, the signal processing performed on the microphone array is equivalent to an acoustic mirror scanning for the detection acoustical waves. The amplitude factor and the phase delay are derived from a propagation model of sound waves. For a medium at rest, which is a suitable assumption for the launch pad environment, the propagation model can be described by the free-field Green's function: $G_{j,m} = \exp(ikr_{j,m})/r_{j,m}$, where $r_{j,m}$ is the distance between the mth microphone and the jth scanning point, and $k = 2\pi f/c$ is the acoustical wave number. Varying the scanning point in space provides a map where the maxima give both the location and the amplitude of the acoustical sources, when they are located in the Fresnel zone of the antenna [10].

The CBM has successfully been used in the past by ONERA at the Martel facility and at full scale on the Ariane 5 launcher. For V503 and V504 flights of Ariane 5, a full microphone array of twelve flush mounted microphones was implemented around the fairing to perform noise source localization. For the flight 503 condition, the map performed with the CBF shows, at the 20 m launcher altitude, one source in the middle of the uncovered central engine flue and two others sources at the SRB flue outlets. In contrast, for the flight 504, the map shows only one source from the central flue, the source radiation from the Solid Rocket Booster flue outlet being strongly reduced by the 30 meter extension flue (Figure 9 from [8]). Recently, a 70-microphone phased array was used to identify noise sources during the Ares I scale model acoustics test. It was found that, using beamforming, the impingement by the plume on various regions of the launch pad constituted the primary noise sources, compared to the free-field configuration [11].

The CBM is an efficient and robust localization technique. It is worth noting that its spatial resolution, measuring the width of the main lobe is proportional to the acoustic wavelength, $\lambda = c/f$. As reminded by Panda and Mosher [12], additionally there may appear multiple local maxima (side lobes), giving the appearance of pseudo noise sources.

DOI: 10.13009/EUCASS2017-38

These difficulties arise from the diffraction characteristics of the array and are dictated by the design of the microphone layout. This property of the array response is described by its point-spread-function, determining how a point source is spread out in the beamforming map. Physically, even the best possible layout of the antenna cannot cancel the side lobes, but only reduce them. The smearing of the actual source location is directly proportional to the frequency of interest: the strength and number of side lobes (that falsely makes the appearance of adjacent sources) is inversely proportional to the frequency. Finally, the CBM may not accurately localize the whole intending sources on the launch pad radiating on the microphone array. The CLEAN-SC, an advanced beamforming routines, was used by Panda and Mosher to image noise source distribution in the plume of a solid rocket motor. The authors observed that while significantly reducing the smearing associated with the point spread function, the CLEAN-SC did not improve resolution beyond that set by the Rayleigh criterion (beamforming is able to separate two noise sources when the first maximum of the secondary source coincides with the first minimum of the primary source).
Nowadays, phase array methods are heavily used in the aircraft industry for the identification of noise sources on airframes, engines, landing gear with recent progress on advanced processing techniques. Additionally, significant advancements in sensor, data acquisition and computing technologies, contribute to improve the sharpening of the noise source distribution. Most of the new processing dedicated to phase array are based on the Deconvolution Algorithm for the Mapping of Acoustic Sources, the so-called DAMAS algorithm technique.

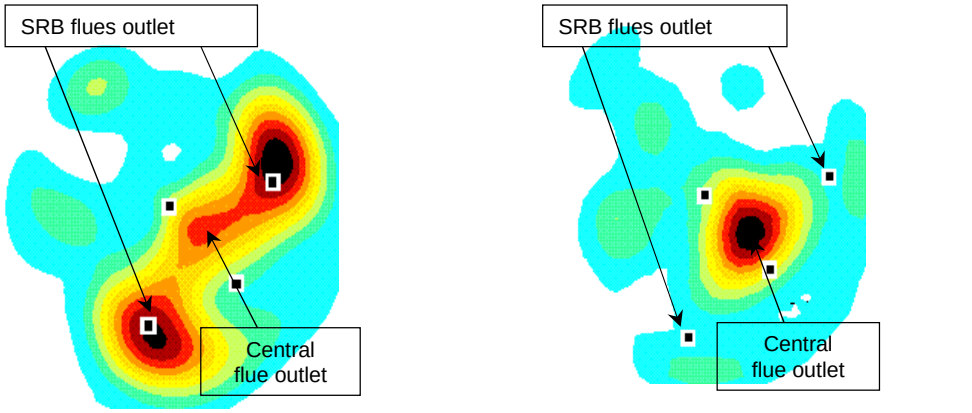

Flight 503 Flight 504, including a flue extension

Figure 9: Maps of the acoustical sources on Ariane 5 launch pad, altitude 20 m [8]

In the aeronautics field, ONERA has successfully applied the DAMAS algorithm to the determination of acoustic directivity from microphone array measurements using correlated monopoles, to the slat noise assessment from Airbus A340 Flyover phased-array microphone measurements, and to landing gear noise sources identification through an application of array methods to experimental and computational data [14], [15], [16]. This section aims to show the capability of the DAMAS method, used for the first time at the Martel facility, to accurately identify the noise source on the mockup of the launch pad of Ariane 6.

3.2 Principle of the advanced DAMAS processing

There have been multiple efforts to improve the array resolution by deconvolving the pointspread function from the beamformed output. The most straightforward one, DAMAS, involves large matrix manipulations and, as a result, very costly computing time. In the following, main mathematical steps for the conventional beamforming and the DAMAS methods are briefly outlined. The DAMAS is based on the algorithm proposed by Brook and Humphreys [13]. The acoustic spectra emitted from the source points are estimated in two stages. First, the phased-array microphone data are analyzed by beamforming. Then, a deconvolution technique is used to remove the so-called point spread function in order to estimate the acoustic source spectra. The DAMAS method can handle both correlated and uncorrelated sources. Due to the heavy computational cost required to apply DAMAS with correlated sources, we consider here the simplest approach with a set of uncorrelated sources. This latter assumption allows performing maps in almost real time. Such a distribution of uncorrelated sources can restitute the mean sound pressure level radiated in the aperture angle of the antenna, but may fail to describe the directivity of the sources radiation in the whole space.
We first briefly remind the CBF formulation in order to introduce the main quantities involved in the DAMAS formulation. In the beam forming approach, s_i, the mean square amplitude of the source at the ith scanning point are expressed as:

DOI: 10.13009/EUCASS2017-38

$$s_i = \sum_{m,n=1}^{N_M} G_{i,m}^{*} \Gamma_{m,n} G_{i,n} \,/ (\sum_{m,=1}^{N_M} G_{i,m}^{*} G_{i,m}) \quad \textbf{(1)}$$

where $G_{i,m}$ is the Green's function between the *i*th scanning point and the *m*th microphone and $\Gamma_{m,n}$ is the cross-spectral matrix of the microphone array. As discussed above, the main limitations of the CBM are the limited spatial resolution and the side lobe in the response of the antenna. This may result in the difficulty to separate close acoustic sources and also to estimate the noise level of the sources.
The DAMAS approach aims to overcome these difficulties by introducing a more realistic *Ns* multi-sources model, to describe the pressure field on the *m*th microphone:

$$p_m = \sum_{j=1}^{N_s} \alpha_j G_{j,m} \quad \textbf{(2)}$$

with $\overline{\alpha_i \, \alpha_j^{*}} = s_i \delta_{i,j}$ for uncorrelated sources. The DAMAS formulation is now summarized below, details of the method can be found in [13]. The principle of the DAMAS approach, like the CBM, is derived from a minimization between a source model and the microphone measurements, *i.e.*, the well-known least mean square method. The DAMAS assumed a set of *a priori* monopole sources distributed in space, as close as possible to the location of the actual sources. The output of the DAMAS approach is to assign the amplitude of these monopoles. *s*, the mean square of the source magnitude is solution of *Hs = b*, *s* under the constraint *s* to be positive (*s >0).* The *H* matrix is defined by:

$$H_{i,j} = \left| K_{i,j} \right|^2 \quad \textbf{(3)}$$

$$\text{where } K_{i,j} = \sum_{m=1}^{N_M} G_{i,m}^{*} G_{j,m} \quad \textbf{(4)}$$

$$\text{and } b_i = \sum_{m,n=1}^{N_M} G_{i,m}^{*} \Gamma_{m,n} G_{i,n} \quad \textbf{(5)}$$

To solve this problem, an iterative algorithm associated with a Tikhonov regularization provides a good balance between accuracy and robustness of the solution [17].

3.3 Array hardware set up at Martel facility

This section reports on the application of a suitably phased array in establishing the noise sources in supersonic hot jet impacting a launch pad. Figure 10 shows the implementation of the 115-microphone array located on the ceiling of the Martel facility. The 115 microphones, Bruel&Kjaer ¼" type, are evenly distributed in a 2mx2m plan, including 5 arms. The microphone array is fixed horizontally on an IPN girder of the Martel structure, directly above the trench at the higher altitude to prevent acoustical disturbance of the pressure field on the fairings. The antenna is located 4.27 m high above the launch table and 1.85 m in lateral from the nozzle exit. To avoid reflections, an acoustical liner is applied on the IPN.
Additionally, a data acquisition and processing system is assembled in the Martel facility, and processing codes are implemented to take advantage of the array procedures. This hardware coupled with efficient algorithms allows providing maps of the CBM and the DAMAS techniques, in almost "real time" during the experiment. The microphone signals of the array are acquired with a commercial system, a B&K LANXI type, at a 131077 Hz sampling frequency, using a dynamic signal provided by a 24 bits digitizing, and high filtered at the 22.4 Hz frequency. Spectra of the cross-spectral matrix are obtained through an average on 300 Fast Fourier Transform of temporal data blocks together with a Hanning weighting. The output processing of the maps are performed on octave bands, from 250 Hz to 16 kHz. Prior to the experiment, an acoustical source was placed on the duct exit to calibrate the 115 channels of the array and to check the expectable functioning of the array response.

DOI: 10.13009/EUCASS2017-38

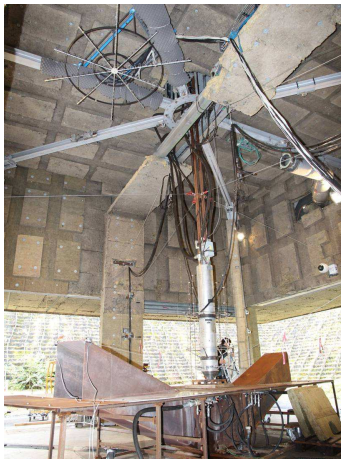

Figure 10: 115-mirocrophone array set up in the Martel facility

3.4 Results

The results from the antenna using the DAMAS processing obtained "in real time" are the maps of the source localization on the trench, as function of the altitude. From among the large amount of processed results, Figure 11 illustrates the maps displayed in a vertical plane containing the jet axis and a set of planes following the trench geometry, in the 4 kHz octave band, and for the launcher altitudes 0 to 35*D*. At zero altitude, as excepted, the entirely acoustical source is found at the trench exit; at 5*D*, the main noise source remains at the duct exit with, in addition, an impact source located directly above the vertical jet; at 20*D*, the duct exit source is significantly reduced, for the benefit of sources located in the vertical jet, additional sources generated by the impacts of the jet on the launch table close trench slope and the reflection of the turbulent mixing noise on the top of the trench; the evolution of the 20*D* behaviour pattern to the 35*D* one, points out a shift of the mixing noise contribution towards the duct exit, in agreement with the 140 degrees radiation direction of this source component (see Figure 8b).

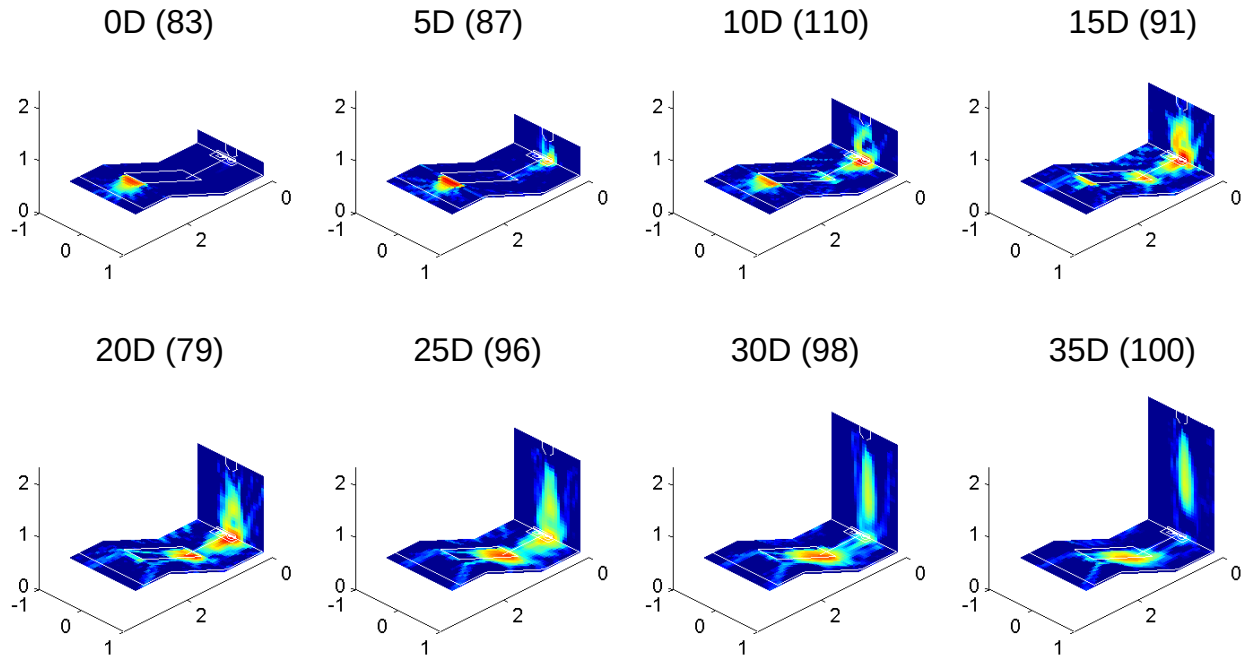

Figure 11: Acoustical maps in the octave band 4 kHz. Top: altitudes 0 to 15*D*; bottom: altitudes 20 to 35*D*

DOI: 10.13009/EUCASS2017-38

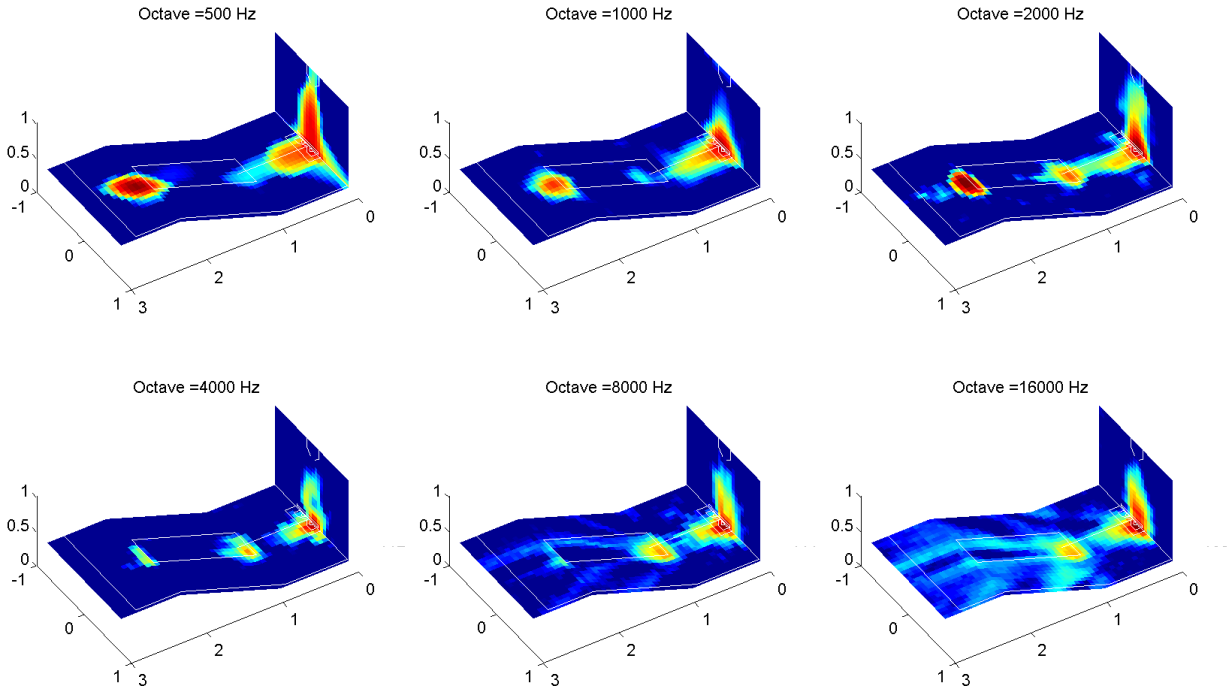

Figure 12: Maps at the altitude 15*D* for the octave bands from 500 Hz to 16 kHz

Figure 12 details the maps at 15*D*, where the maximum of the SPL radiated occurs, as function of the frequency. Roughly speaking, it appears that in the low frequency range, from the octaves 500 Hz to 2 kHz, the dominant sources are located on the duct exit, on the impact of the jet and in the vertical plane, while from 4 kHz to 16 kHz, a source at the foot of the trench slope is also present.

As a complementary analysis, the powerful interest of the DAMAS is its capability to determine the deconvolved noise levels to be integrated over specific domains, in order to get the acoustic power contribution emitted from sub-areas. Figure 13 illustrates a proposed decomposition of the vertical and horizontal planes into noise sources: vertical jet (orange area), jet impact with the launch table (red area), turbulent mixing zone (green area), trench exit (blue area). Theoretically, using an uncorrelated noise source distribution in the DAMAS formulation, such domain decomposition enables to determine the contribution of the acoustical sources to the pressure field radiated on the aperture angle of the antenna. Using correlated noise source assumption in the formulation, requiring heavy CPU time resource, would also provide an unbiased sample of the radiated field on the fairing.

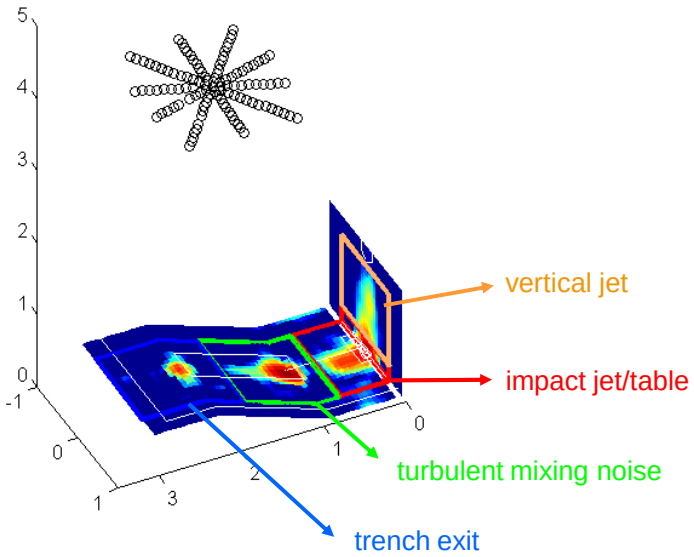

Figure 13: Decomposition of the noise source zones (black circles represent the microphones)

DOI: 10.13009/EUCASS2017-38

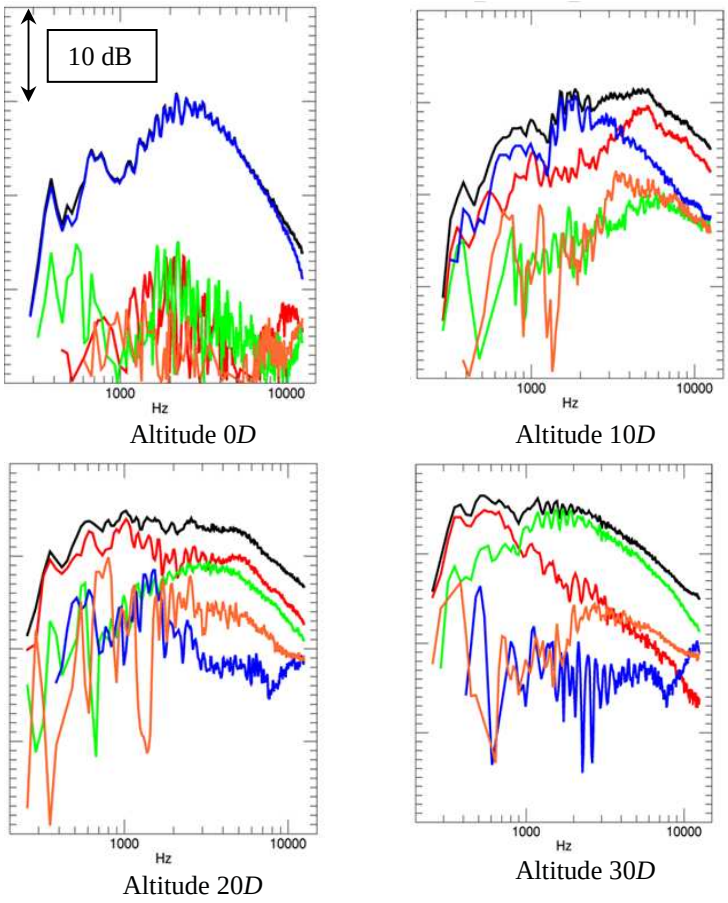

Figure 14: Deconvolued density spectral level from the source zones.

(-) total pressure; (-) trench exit; (-) impact jet; (-) vertical jet; (-) turbulent mixing noise

Figure 14 shows the deconvolued density spectral levels radiated on the microphone location from the source zones, at four altitudes. The black curve represents the total pressure, while the other curves colors match with the zones color defined in Figure 13. At 0*D*, it is found that the main contribution to the radiation comes from the zone at the trench exit; at 10*D*, an allocation between the trench exit and the impact jet zones appears, depending on the frequency; at 30*D*, the impact source is dominating in the low frequency range, while the turbulence mixing noise mainly contributes to the pressure level in the higher frequency range. Generally speaking, the DAMAS output allows to identify and to rank the noise source components, which is of strong interest to investigate the performance of reduction devices.

5. Semi-empirical predictions

Engineering models based on semi-empirical prediction with correlations to scaled measurements are the current state-of-the-art production tools. Belonging to this kind of model, Minotaure is a code developed at ONERA for the prediction of hot supersonic jet [18]. It is based on the Eldred's model where the acoustical power, representing less than a 1% of the kinetic power of the engines, is distributed on monopole sources along the jet axis [5]. It is to notice that the initial Eldred's semi-empirical approach developed in 1971, has been enhanced during the last years. Especially, Varnier has proposed a half-length of the plume potential core, a sensitive parameter in the Eldred's model [19]. In 2009, modifications of the Eldred's formulation have been achieved for Ares I lift-off environment predictions, including the shorter core length approximation, a core termination procedure upon plume deflection and a new set of directivity indices derived from measurements [20]. While recent progressing CFD can handle free supersonic hot jet or jet impinging on academic shape obstacles, the semi-empirical approach still remains an efficient tool to predict the environment of launcher with the complex geometry of a launch pad, under controlled margin errors.

DOI: 10.13009/EUCASS2017-38

Compared to the initial Eldred's formulation, Minotaure takes into account the penetration of the jet into the trenches including a sound attenuation and the reflections of the acoustic waves on the launch pad. Minotaure splits up the acoustical power into two jets: one penetrating into the trench and the other one bursting out on the launch table and on the ground. The balance of the acoustical power between the two jets depends on the altitude of the launcher. At low altitude, most of the energy is associated to the jet inside in the trench and, typically from 20*D* altitude, the energy is allocated to the impinging jet. Figure 15 illustrates the jets modelization in Minotaure for the mockup of the Ariane 6 launch pad set in the Martel facility.

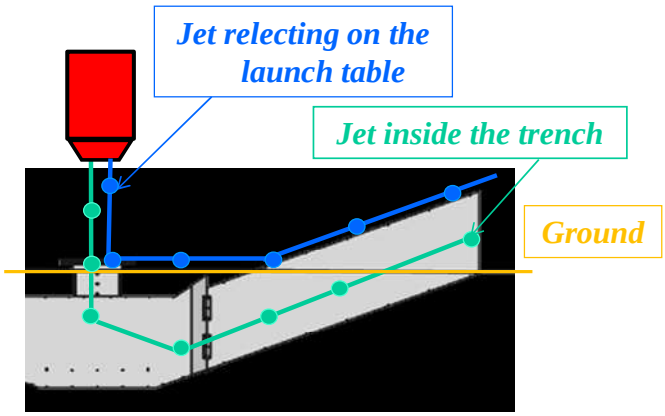

Distribution into two jets of the jet at the inlet exit

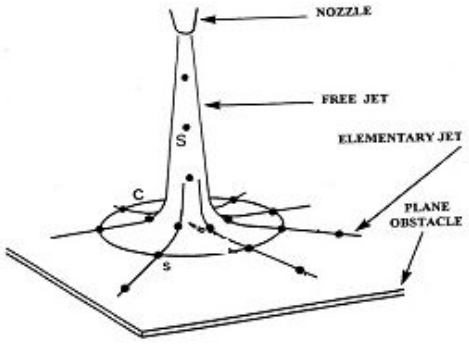

Detail view of the jet reflecting on the ground

Figure 15: Jets modelization in Minotaure for the mockup of the Ariane 6 launch pad

5.1 Results on the mockup of the launch at Martel facility

The first predictions with Minotaure concern the configuration on the scaled mockup at Martel facility, using the aero-thermodynamics inputs of the jet, with the cone-shaped convergent-divergent nozzle. Figure 16 shows the comparison between the Martel measurement and the Minotaure prediction. Minotaure and measurement results are average from the microphones located on the G4 and G5 rings. It is observed in Figure 16a that, the overall shape of the measurement is satisfactory found with Minotaure, including a strong reduction at zero altitude when the trench fully operates and a maximum of the sound pressure close to the 15-20*D* altitude, with a systematic underestimation of the pressure at all the altitudes. This underestimation also appears at 35*D* where the free jet radiation can be assumed. Such a behavior already occurred in the past. It is believed that Minotaure is applied out of its application domain: the indices directivity associated to the sources along the jet axis implemented in Minotaure and derived from the Eldred's formulation in free field are calibrated for observation points in the far field that does not reach the very upstream locations of the G4 and G5 strings. The agreement of the spectra is quite good in the high frequency range but the prediction underestimated the level in the low frequency part. Such a deviation suffers from the absence of modifications of the model indices sources that can arise, with the jet penetration in the trench.

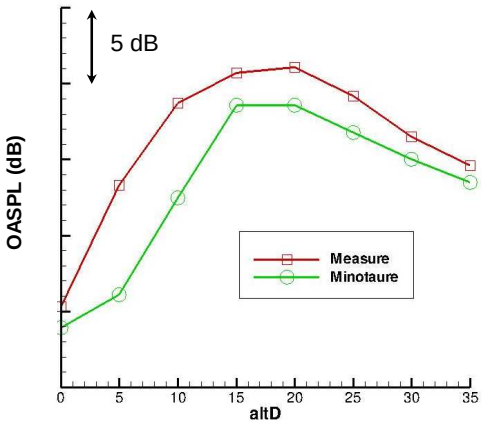

a) Over All Sound Pressure level.

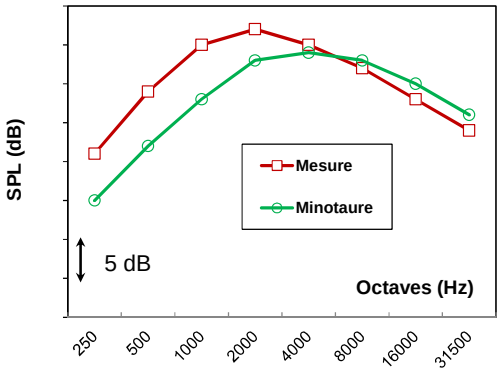

b) Spectra at the altitude 20*D*.

Figure 16: Comparisons between Martel measurements and Minotaure predictions

DOI: 10.13009/EUCASS2017-38

The Minotaure accuracy was assessed against well-controlled configurations at reduced scales, especially in the ADEL research. The above results confirm the same margin error. Minotaure can also handle water injection. However, the configurations studied to calibrate the water effect (trench geometry and water injection location) are too far from those of the present Martel campaign to provide a reliable sound reduction. The tool cannot be applied in proactively designing launch pad topology modifications or targeted placement of sound suppression water flow for maximum acoustic load mitigation effects. More detailed modeling approaches are needed to identify the sources of noise generation and the effects of sound mitigation efforts. Additional model work and data base from measurements are required to achieve this objective. In practice, the influence of the water injection in the predictions is straightforwardly derived from the reduction measured in the Martel facility (see Figure 7).

5.2 Prediction on the Ariane 5 and Ariane 6 launch pads at full scale

Figure 17 illustrates the launch pad of Ariane 5 and to Ariane 6 at full scale. For Ariane 5 two covered trenches (orange colored) are considered to guide the jet by the two solid rocket engines (presented with green disks) and the central jet generated by the cryogenic engine (presented with the blue disk) is guide by an open trench (magenta colored). For Ariane 64 (configuration of Ariane 6 with 4 lateral boosters) two trenches both guide the jets of the 4 solid rocket engines and the jet from the cryogenic engine; the jets are splitted into the two trenches. The Minotaure predictions require the aero-thermodynamic inputs of each engine. No interactions between the jets are introduced, so that the total acoustical power considered is derived from the summation of each engine contribution.

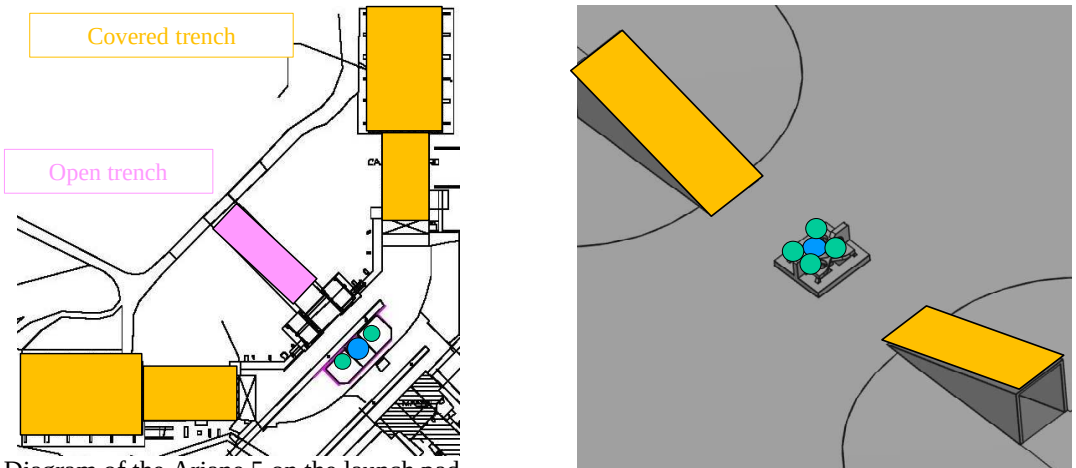

Diagram of the Ariane 5 on the launch pad

Diagram of the Ariane 6 on the launch pad

Figure 17: Launch pads of Ariane 5 and Ariane 6 (magenta: open trench, orange: covered trench)

Figure 18 compares the Minotaure predictions for Ariane 5 and Ariane 6. As expected from the Martel predictions, a very significant reduction is confirmed at low altitudes for Ariane 6, due to the efficiency of the deep and long trenches. In contrast, the Ariane 5 prediction exhibits a higher sound pressure level due to the radiation at the ignition of the cryogenic engine at low altitude.

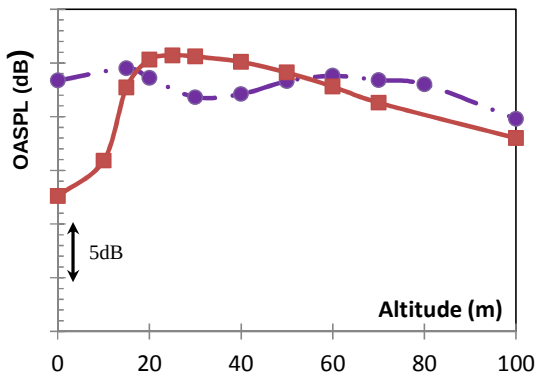

Figure 18: Minotaure predictions: (●) A5; (■) A64

DOI: 10.13009/EUCASS2017-38

6. Conclusion

In the framework of the future Ariane 6 launcher, the characterization of the jet noise on the launch pad was performed to control the pressure level on the payload, at lift-off. The launch pad consists of two covered long trenches guiding both the jets generated by the solid rocket boosters and the main cryogenic engine. The acoustical characterization was conducted through a tests campaign carried out at the MARTEL facility, with a mockup of the launch pad at 1/40-scale. It is found from the microphone on the payload, that the covered trenches strongly attenuate the level at low altitudes, and that the maximum of the sound pressure level is reached at about a 20D altitude of launcher, D being the nozzle diameter. A 115-microphone phase array provides an accurate spatial resolution of the noise sources on the launch pad, using the DAMAS method. This efficient tool confirms that at low altitudes the noise radiation comes from the trenches exit, and shows that the maximum of the sound pressure at 20D comes from the combination of the turbulent mixing noise component reflecting on the trench roofs and additional sources, coming from the impingement of the jet plume on the launch pad. Additionally, the DAMAS technique enables to rank and to quantify the noise sources contribution to the radiated sound pressure level. Future works should concern the application of the DAMAS algorithm using correlated sources to reproduce the directivity of the source on the launch and to accurately describe the radiation of these sources on the fairing itself, while using uncorrelated, the radiation domain is restricted to the aperture angle of the microphone array. The semi-empirical predictions from Minotaure, at the 1/40-scale, show a good agreement with the Martel experiment, finding at low altitudes the strong attenuation provided by the long trench. Improvements on the predictions could include the complex modelization of the influence of the water injection.
The view expressed in the paper can in no way be taken to reflect the official opinion of the European Space Agency.

Acknowledgements

The authors would like to thank the European Space Agency for supporting this study and also CNES for fruitful interactions during the technical activity. They also thank the technical staff from the MARTEL facility for their efficient contribution during the campaigns.

References

[1] Varnier, J., P. Prévot, G. Dunet, M. Barat, and B. Mazin. 2006. Blast wave and afterburning at ignition of rocket engines. In: *13th International Congress on Sound and Vibration*, ICSV13, 2-6 July, Vienna, Austria.

[2] Bresson, C., H. Foulon, H. Lambaré, M. Pollet, P. Malbéqui. 2011. A blast wave generator in MARTEL facility to simulate overpressure induced by solid rocket motor at lift-off. In: *4th European Conference for Aerospace Sciences*, EUCASS, 4-8 July, Saint-Petersburg, Russia.

[3] Tam, Ch. K. W. 1995. Supersonic jet noise. In: *Annu. Rev. Mech.* 27: 17-15.

[4] Seiner, J.M., M. K. Ponton, B. J. Jansen, N.T. Lagen. 1992. The effects of temperature on supersonic jet noise emission. AIAA Paper 92-02-046.

[5] Eldred, K., 1971. Acoustic Loads Generated by the Propulsion System. In: *NASA SP-8072*, June 1971.

[6] Jouy, B., J. Troyes, J.-B. Dargaud, and F. Vuillot. 2011. Numerical simulation of the overpressure at Martel facility: combustion and wave generation. In: *4th European Conference for Aerospace Sciences*, EUCASS, 4-8 July, Saint-Petersburg, Russia.

[7] Troyes, J., F. Vuillot, H. Lambaré, A. Espinosa Ramos. 2015. Study of impinging supersonic jet noise with aerodynamics and acoustics numerical simulations. In: *30th International Symposium on Space Technology and Science*, 2015-399, Kobe-Hyogo, Japan.

[8] Gély, D., G. Elias, C. Bresson, H. Foulon, and S. Radulovic. 2000. Reduction of supersonic jet noise: application to the Ariane 5 launch vehicle. In: *6th AIAA/CEAS Aeracoustics Conference*, 12-14 June, Lahaina, USA.

[9] Espinosa Ramos, A., Hiverniau B. 2015. ADEL Research Group. In: *30th ISTS Congress, launch Vehicle acoustics session*, 4-10 July, Kobe-Hyogo, Japan.

[10] Elias, G and C. Malarrmey. 1983. Utilisation d'antennes focalisées pour la localisation des sources acoustiques. In: *11ème congrès International d'Acoustique*, 19-27 Juillet, Paris, France.

[11] Panda, J., R. Mosher. 2013. Microphone phased array to identify liftoff noise sources in model-scale tests. In: *Journal of spacecraft and Rockets*, Vol. 50, No. 5, September–October 2013.

[12] Panda, J., R. Mosher. 2011. Use of a Microphone Phased Array to Determine Noise Sources in a Rocket Plume. In: *49th AIAA Aerospace Sciences Meeting including the New Horizons Forum and Aerospace Exposition*, AIAA 2011-974, 4-7 January 2011, Orlando, Florida.

DOI: 10.13009/EUCASS2017-38

[13] Brooks, T. F., W. M. Humphreys. 2005. A deconvolution approach for the mapping of acoustic sources (DAMAS) determined from phased microphone arrays. In: *J. Sound Vib*. 294, 856–879.
[14] Fleury, V., J. Bulté, R. Davy. 2008. Determination of acoustic directivity from microphone array measurements using correlated monopoles. In: *14th AIAA/CEAS Aeroacoustics Conference*, AIAA 2008-2855 (2008).
[15] Fleury, V., P. Malbéqui. 2013. Slat Noise Assessment from Airbus A340 Flyover Phased-Array Microphone Measurements. In: *AIAA Journal*, Vol. 51, N°7, July 2013.
[16] Redonnet, S., J. Bulté. 2016. Landing gear noise sources identification through an application of array methods to Experimental and computational data. In: *22nd AIAA/CEAS Aeroacoustics Conference*, AIAA 2016-2844, 30 May-1 June, Lyon, France.
[17] Shafer, R., R. Mersereau, M. Richards. 1981, Constrained iterative restoration algorithms. In: *Proc. IEEE*, 69, 432-450 (1981).
[18] Gounet, H. 2010. Evaluation de l'environnement sonore des lanceurs au décollage. In: *10ème Congrès Français d'Acoustique*, 12-16 avril 2010, Lyon, France.
[19] Varnier, J. 1998. Noise radiation from free and impinging hot supersonic jets. AIAA Paper 98-2206.
[20] Haynes, J., R. J. Kenny. 2009. Modifications to the NASA SP-8072 distributed source method II for Ares I lift-off environment predictions. In: *15th AIAA/CEAS Aeroacoustics Conference (30th AIAA Aeroacoustics Conference)*, AIAA 2009-3160, 11-13 May 2009, Miami, Florida, USA.